

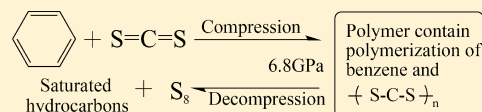
Carbon Disulfide Assisted Polymerization of Benzene

Mi Zhou, Zhanlong Li, Zhiwei Men, Shuqin Gao, Zuowei Li, Guohui Lu, and Chenglin Sun*

State Key Laboratory of Superhard Materials, College of Physics, Jilin University, Changchun 130012, China

S Supporting Information

ABSTRACT: The chemical transformation of benzene (C_6H_6) and carbon disulfide (CS_2) binary solution under high pressure condition is investigated by means of Raman spectroscopy up to 6.8 GPa. On increasing the pressure, all the Raman bands of benzene decrease in intensity, whereas new broad bands start to be observed at 1520 and 1450 cm^{-1} , indicating that a highly cross-linked polymer is formed. The recovered sample is analyzed through Raman and FT-IR spectroscopy and is identified as a saturated hydrocarbon and element sulfur.



1. INTRODUCTION

High pressure research of organic compounds has attracted great interest in the past two decades;^{1–5} among organic compounds, reversible and irreversible transformations are frequently observed. Irreversible transformations generally occur in unsaturated bond systems^{6–11} since application of high external pressure can induce intermolecular and intramolecular interaction comparable in magnitude, making the new opportunity in the synthesis of new materials, such as conductive polymers, wideband gap semiconductors, and super hard amorphous solids.^{12–14} The unsaturated bond system under investigation always contains unsaturated double or triple carbon–carbon bonds, aromatic rings, and heterocycles. When pressure is increased to a certain critical value, completely amorphous products can be obtained.^{15,16} The details of such reaction mechanisms, particularly the interdependence between the compression of intermolecular contacts and molecular deformations, are still not clear. Meanwhile, this information is crucial for understanding the structural features of the pressure-induced polymerization.

Among the compounds of unsaturated systems, benzene is the prototype of the aromatic compounds, and its phase and chemical transformation under pressure is one of the most extensively studied examples.^{16–21} Theoretically, several high-pressure benzene phases are predicted by X. Wen, R. Hoffmann, and N. W. Ashcroft.²² The recent phase diagram of benzene, drawn on the basis of different spectroscopic investigations, reports six different crystal phases.^{23–26} As the pressure and temperature are raised, crystalline benzene undergoes irreversible chemical reactions, and the products vary widely by employing specific experimental conditions. At room temperature, the pressure-induced chemical transformation is observed at around 23 GPa, and the reaction pressure can be lowered down to 16 GPa if a suitable laser is applied to the sample.²⁷ The purpose of this article is to lower the threshold pressure for the chemical transformation of benzene.

In the present work, we investigate the high-pressure behavior of C_6H_6 – CS_2 binary solution up to 6.8 GPa in a diamond anvil cell by Raman spectroscopy. A detailed analysis

of the Raman scattering and infrared absorption spectra is performed on the recovered products. The experimental results indicate that the aromatic ring of benzene polymerizes after a compression-release cycle, and the final products have the characteristics of saturated hydrocarbons and element sulfur.

2. EXPERIMENTAL METHODS

Benzene and carbon disulfide are purchased from Sigma Aldrich and used without further purification. The high-pressure cell used in this experiment is based on a symmetric diamond anvil cell (DAC) having two diamonds with 500 μm culet size. The sample with a small ruby chip ($\sim 10 \mu m$) is loaded in a 200 μm hole drilled in a 250 μm thick T301 gasket preindented to 80 μm thickness. The pressure calibration is done using ruby fluorescence.²⁸ No pressure-transmitting liquid medium is used in the experiment. We monitor the separation between the R_1 and R_2 components of the ruby fluorescence line, which is found to remain invariant even at the highest pressure, indicating a negligible nonhydrostatic component. The Raman spectra are recorded using a Renishaw in Via Raman Microscopic instrument. Laser excitation at 514.5 nm is obtained with a Spectra Physics 160 M argon ion laser. A Leica microscope with $\times 50$ objective lenses enables measurements with backscattering geometry. The laser power is 3.6 mW, and the typical accumulation time for each spectrum is 30 s. Frequency calibration of the Raman spectrum is realized using the characteristic 520 cm^{-1} line of silicon. All measurements are conducted at room temperature. An FT-IR spectrum of the recovered sample is recorded at room temperature by a Nicolet 360 equipped with a DTGS detector at a resolution of 4 cm^{-1} , scan range 400–4000 cm^{-1} , and scanned 320 times.

3. RESULTS AND DISCUSSION

3.1. High Pressure Raman Spectroscopy of Benzene and Carbon Disulfide Binary System. Figure 1 shows the Raman spectra of C_6H_6 – CS_2 binary system, with 0.3 volume

Received: December 12, 2011

Revised: February 2, 2012

Published: February 6, 2012

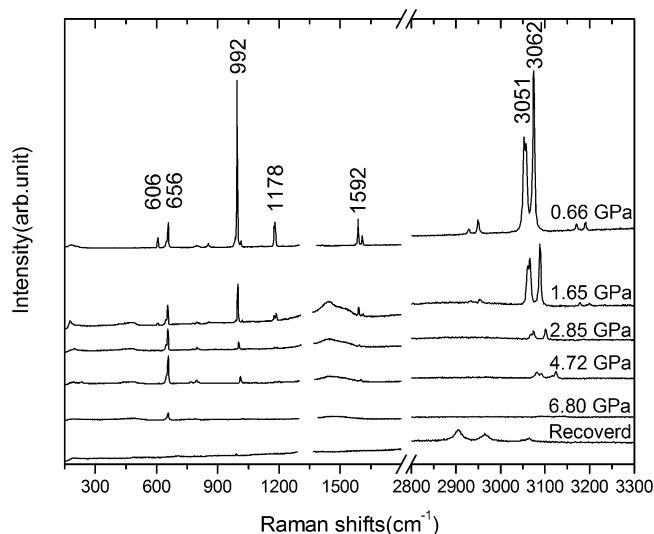


Figure 1. High-pressure Raman spectra of $\text{C}_6\text{H}_6\text{-CS}_2$ binary system.

fraction of CS_2 , at selected high pressures carried out up to 6.8 GPa. Because of the edge filter, we are unable to observe any low-frequency mode below 120 cm^{-1} .

The Raman band located at 656 cm^{-1} is attributed to the C–S symmetric stretching vibration of carbon disulfide,²⁹ the 992 cm^{-1} Raman line is assigned to the ring breathing vibration of benzene.³⁰ In the pressure range from ambient pressure to 4.7 GPa, the intensity of 656 cm^{-1} has an approximately constant value, while all the Raman bands of benzene decreased in intensity significantly during the compression process, suggesting that the content of benzene is decreasing with pressure. Figure 2 displays a relationship between the Raman intensity of

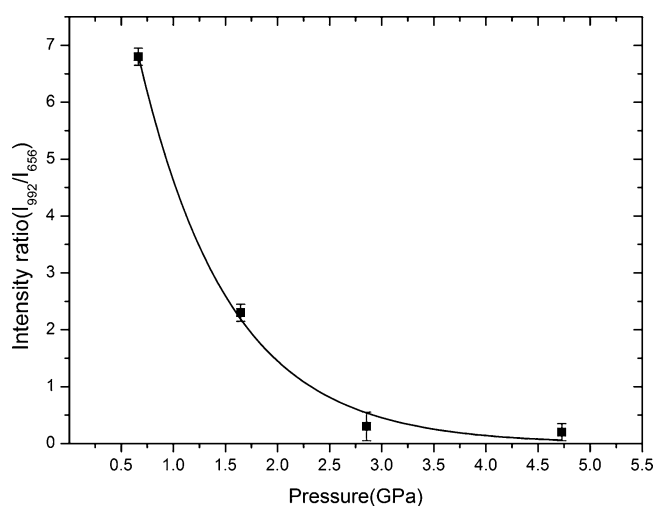


Figure 2. Relationship between intensity ratio of 992 cm^{-1} to 656 cm^{-1} bands and pressure.

the 992 cm^{-1} and 656 cm^{-1} bands; the solid line is a simple exponential fitting to the data points, indicating that the chemical transition rate of benzene is linear proportional to the external pressure. At 1.65 GPa, new broad peaks centered at 1450 and 1520 cm^{-1} appear in the Raman spectra of $\text{C}_6\text{H}_6\text{-CS}_2$ binary solution; the broad bands have characteristics of disordered polymers. The 1520 cm^{-1} Raman band may belong to the G band of hydrocarbons, which contain five or six-membered rings,^{31–33} as a result of the chemical transformation

of benzene and carbon disulfide. They could be thought of as multidimensional arrays of C_6H_6 rings bridged to each other by carbon disulfide or dearomatized benzene.^{22,34} During the polymerization process, direct polymerization formed by benzene–benzene may occurs; it depends on the distance and orientation between C atoms on the nearest-neighbor molecules. Assuming that the molecular orientations do not change with pressure, the benzene–benzene polymerization occurs when the distances are comparable to or greater than the van der Waals separation.²⁶ The 1450 cm^{-1} band may be ascribed to the $(\text{-S=C-S-})_n$ asymmetric stretching mode of polymeric CS_2 , and a similar Raman peak is observed for neat carbon disulfide under compression [Supporting Information, S2]. In the pressure range from 4.7 to 6.8 GPa, the intensity of the two broad bands and 656 cm^{-1} Raman line decrease rapidly with increasing pressure and finally disappear, suggesting that a high cross-linked polymer is obtained as a result of the instability of carbon disulfide. The reaction of carbon disulfide with organic compounds under compression has been investigated before.^{35,36} Carbon disulfide has been extensively investigated by various spectroscopic techniques at high pressure.^{37,38} It is crystallized at 295 K and 1.26 GPa to give an orthorhombic structure; no phase transitions occur with further increasing pressure until the black polymerization onset at 8 GPa.

In the high wavenumber region ($3000\text{--}3150\text{ cm}^{-1}$), the intensity enhancement of ν_7 (e_g) C–H asymmetric stretching peak on the ν_2 's low frequency side is an evidence of significant intermolecular coupling (C–H/ π) between adjacent molecules at high pressure. The evolution of the C–H stretching band as pressure increases indicates a continuous chemical transformation from the high pressure species toward a system composed of a highly cross-linked polymer.

3.2. Frequency-Pressure Relationship of Benzene and Carbon Disulfide Binary System. Comparative high-pressure Raman spectra of benzene, carbon disulfide, and their binary solution are shown in Figure 3. There is a monotonic increase in their Raman mode frequency throughout the compressed process, the frequency–pressure relationships are plotted in Figure 4, and the slopes of the frequency–pressure curve are given in Table 1. It can be noticed that the slope of the 656 cm^{-1} Raman line of neat CS_2 is higher than that of its benzene binary solutions. On the contrary, the slopes of 606 , 992 , 1178 , 1592 , 3051 , and 3062 cm^{-1} Raman bands of neat benzene are lower than those of its carbon disulfide binary solutions. These spectroscopic phenomena demonstrate that CS_2 is more rigid than benzene. Compared with neat benzene, in $\text{C}_6\text{H}_6\text{-CS}_2$ binary solution, benzene is more sensitive to compression and makes a major contribution to the reduction of volume. It may be the main reason that the chemical transformation of benzene begins to occur at a relatively low external pressure. For comparison purposes, high pressure Raman spectroscopic investigations are also carried out on benzene–carbon disulfide binary solution with 1:1 volume ratio. The frequency–pressure slopes of 606 , 992 , 1178 , and 1592 cm^{-1} Raman bands in 3:7 volume ratio solution are larger than those in the 1:1 volume ratio solution. On the contrary, the 3051 and 3062 cm^{-1} Raman bands, which are attributed to the asymmetric and symmetric C–H stretching vibration, respectively, show the opposite tendency. We believe those C–H frequency–pressure behaviors have a strong correlation with benzene–benzene C–H $\cdots\pi$ interactions on the basis of the electron–phonon coupling effect. The intermolecular C–H $\cdots\pi$

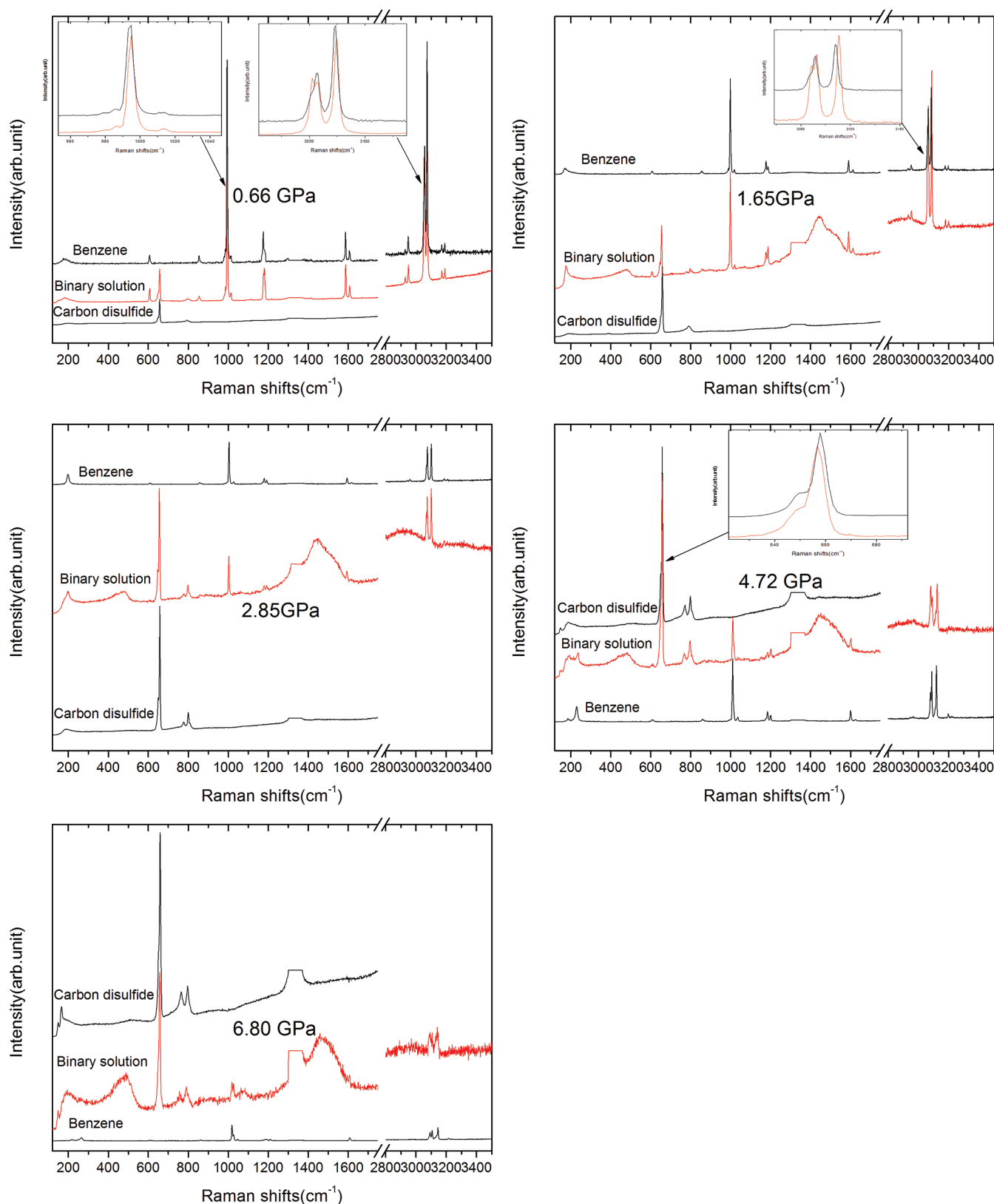


Figure 3. High-pressure Raman spectra of benzene, carbon disulfide, and their binary solution.

attractive force in the 3:7 volume ratio solution is stronger than that in the 1:1 volume ratio solution, and this might be the main reason for the C–H frequency–pressure phenomena. After a compression–release cycle, similar recovered products can be obtained from the two binary solutions.

3.3. Recovered Products of Benzene and Carbon Disulfide Binary Solution under Pressure up to 6.8 GPa. After the DAC is opened, three rod-shaped samples appear in the transparent environment. Besides, they are stable under ambient conditions, and the visual observation of the recovered

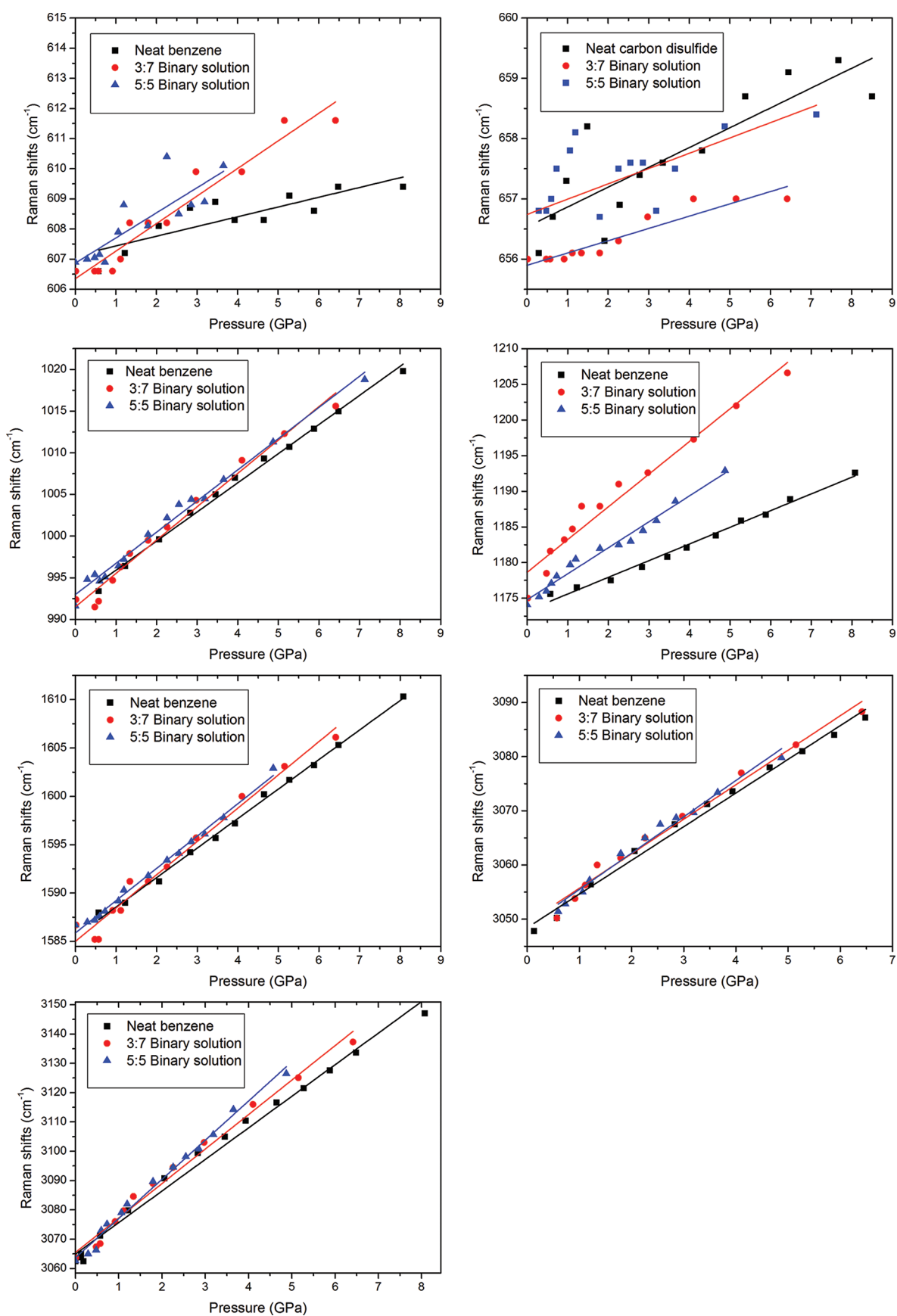


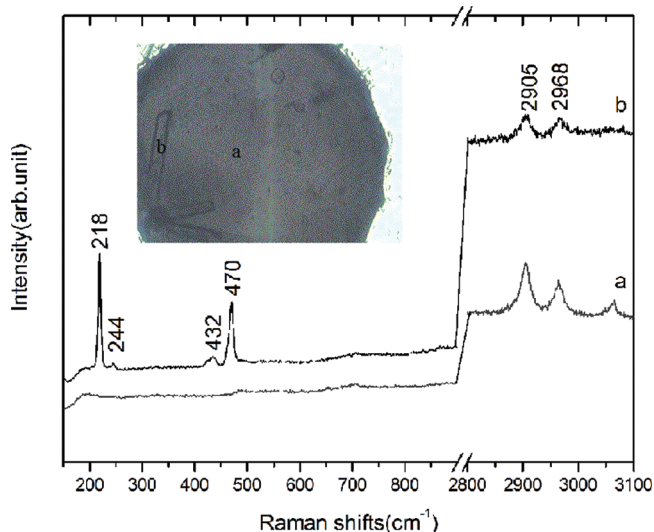
Figure 4. Plots for frequency–pressure relationships.

Table 1. Mode Frequencies (ω), Pressure Derivatives ($d\omega/dp$) of Selected Raman Modes^a

bands (cm ⁻¹)	neat benzene	benzene in CS ₂ (70%)	benzene in CS ₂ (50%)	neat CS ₂
606	0.32	1.02	0.81	
656		0.18	0.25	0.38
992	3.61	3.97	3.74	
1178	2.34	4.85	4.15	
1592	3.05	3.61	3.32	
3051	5.72	6.02	6.71	
3062	10.77	12.07	13.40	

^aMode number and assignments are based on refs 29 and 30.

samples in DAC is shown in Figure 5. The Raman spectra of rods and transparent areas are also given in Figure 5. As the

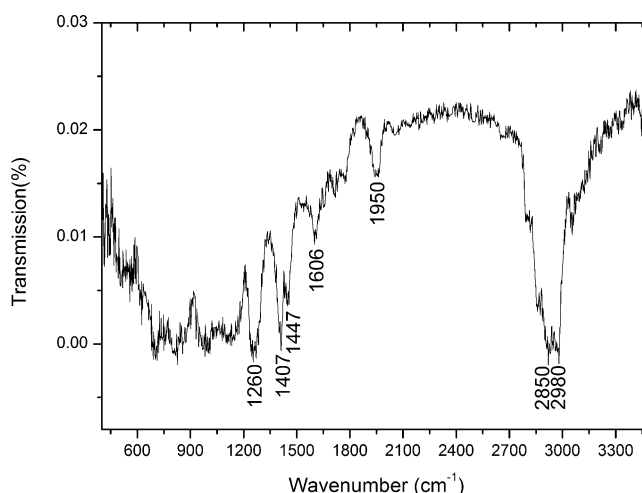
**Figure 5.** Visual observation and the Raman spectra of the recovered products (a, transparent environment; b, rod-shaped S₈).

rods are immersed into the transparent environment, their Raman spectra contain the same bands located at 2905 and 2968 cm⁻¹, which are attributed to the C–H stretching vibration of CH₂ and CH₃,³⁹ indicating that saturated hydrocarbons are formed in the release process. In the binary solution, the coupling of unsaturated molecules at high pressure may occur through π bonds. Consequently, these bonds are strongly affected, and the stability condition of the aromatic ring is likely no longer fulfilled. The destabilization of the aromatic ring may lead to either (a) formation of saturated bonds by coupling between carbons of adjacent molecules or (b) hydrogen migration and formation of CH₂ groups. Under compression, this transformation seems to be gradual and could be understood in the case that hydrogen migration increases as the pressure decreases. This suggests that saturated CH phases are favored thermodynamically over molecular structures (benzene crystals) at high pressure.

For rod-shaped samples, strong sharp bands are observed at 218, 244, 432, and 470 cm⁻¹, which are consistent with the typical Raman spectra of S₈,^{40–42} suggesting element sulfur is one of the products of C₆H₆–CS₂ binary solution in this transformation. However, by comparing the two binary solutions of volume ratio of 3:7 and 1:1, bar-shaped S₈ only appears in 3:7 volume ratio solution. This may be due to a

complicated solvent effect in high concentrated solution, which is not suitable for the growth of element sulfur.

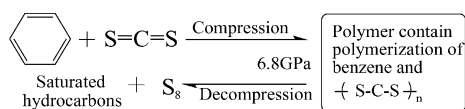
3.4. FT-IR Spectrum of Recovered Products. The FT-IR spectrum of the recovered products is shown in Figure 6, and

**Figure 6.** FT-IR spectrum of the recovered products.**Table 2. Assignments of FT-IR Spectra of the Recovered Sample**

number	frequency (cm ⁻¹)	assignments ⁴³
1	1260	δ_s -CH ₃
2	1407	δ_{as} -CH ₃
3	1447 and 1606	carbon six-membered rings
4	1950	–C=C=C– stretching
5	2850–2980	–CH ₃ and –CH ₂ – stretching

tentative assignments are given in Table 2. An intense broad band appears in the 2850–2980 cm⁻¹ region, consistent with its Raman spectrum, which is the saturated C–H (–CH₃ or –CH₂–) stretching band. The infrared absorption peak at 1950 cm⁻¹ is attributed to the –C=C=C– stretching vibration. The carbon six-membered ring C=C stretching bands can be observed at 1606 and 1470 cm⁻¹, suggesting the products contain (unsaturated C–C bonds) sp² carbon bonds, this may arise from incomplete saturation of the compound or be a segment of polymerization. The absorption bands at around 1250 and 1407 cm⁻¹ may be assigned to the symmetric and asymmetric δ -CH₃ vibration. In the infrared region between 400–1000 cm⁻¹, the spectrum consists of overlapping weak bands, and it is difficult to draw exact peaks position associated with S₈.

As may be expected from the experimental results, under compression, unsaturated C–S bonds and, especially, aromatic bonds may be destabilized to form a denser polymer. After the pressure is released, the recovered compounds with saturated bonds are obtained. Because of the small mass of the recovered sample, it is difficult to draw a precise conclusion concerning the molecular species involved in this transformation, the recovered samples may be composed of crystallites and amorphous zones of various relative dimensions, and a possible reaction path was proposed based on the above analysis.



CONCLUSIONS

The present work provides evidence for such a chemical transformation in benzene–carbon disulfide binary solution after static pressurization up to 6.8 GPa, at room temperature. Detailed analysis about the Raman scattering and FT-IR absorption spectra suggests that the aromatic ring is changed after a compression–decompression cycle, the entire transformation involves a ring polymerization, and the final products must be composed of saturated carbon structures and element sulfur. This article provides experiments employing the solvent-assisting method, which is an efficient way to lower the critical pressure of the polymerization of benzene.

ASSOCIATED CONTENT

Supporting Information

Experimental details; high-pressure Raman spectra of benzene–carbon disulfide binary solution and selective high-pressure Raman spectra of carbon disulfide. This material is available free of charge via the Internet at <http://pubs.acs.org>.

AUTHOR INFORMATION

Corresponding Author

*E-mail: mzhou@jlu.edu.cn.

Notes

The authors declare no competing financial interest.

ACKNOWLEDGMENTS

This work is supported by the National Science Foundation of China (Grant No. 10974067 and 11104107), as well as Ph.D. Programs Foundation of Ministry of Education of China (Grant No. 20110061120008), and the China postdoctoral science Foundation (Grant No. 20110491320).

REFERENCES

- Beer, L.; Brusso, J. L.; Haddon, R. C.; Itkis, M. E.; Kleinke, H.; Leitch, A. A.; Oakley, R. T.; Reed, R. W.; Richardson, J. F.; Secco, R. A.; Yu, X. *J. Am. Chem. Soc.* **2005**, *127*, 18159–18170.
- Chapman, K. W.; Halder, G. J.; Chupas, P. J. *J. Am. Chem. Soc.* **2009**, *131*, 17546–17547.
- Lamelas, F. J.; Dreger, Z. A.; Gupta, Y. M. *J. Phys. Chem. B* **2005**, *109*, 8206–8215.
- Olejniczak, A.; Ostrowska, K.; Katrusiak, A. *J. Phys. Chem. C* **2009**, *113*, 15761–15767.
- Hernandez, I.; Gillin, W. P. *J. Phys. Chem. B* **2009**, *113*, 14079–14086.
- Wilhelm, C.; Boyd, S. A.; Chawda, S.; Fowler, F. W.; Goroff, N. S.; Halada, G. P.; Grey, C. P.; Lauher, J. W.; Luo, L.; Martin, C. D. *J. Am. Chem. Soc.* **2008**, *130*, 4415–4420.
- Fanetti, S.; Citroni, M.; Bini, R. *J. Chem. Phys.* **2011**, *134*, 204504.
- Jennings, E.; Montgomery, W.; Lerch, P. *J. Phys. Chem. B* **2010**, *114*, 15753–15758.
- Chelazzi, D.; Ceppatelli, M.; Santoro, M.; Bini, R.; Schettino, V. *J. Phys. Chem. B* **2005**, *109*, 21658–21663.
- Sakashita, M.; Yamawaki, H.; Aoki, K. *J. Phys. Chem.* **1996**, *100*, 9943–9947.
- Murli, C.; Song, Y. *J. Phys. Chem.* **2010**, *104*, 9744–9750.
- McMillan, P. F. In *High-Pressure Crystallography*; Katrusiak, A., McMillan, P. F., Eds.; Kluwer: Dordrecht, The Netherlands, 2004; pp 367–392.

- Solozhenko, V. L. In *High-Pressure Crystallography*; Katrusiak, A., McMillan, P. F., Eds.; Kluwer: Dordrecht, The Netherlands, 2004; pp 411–428.
- McMillan, P. F. *Nat. Mater.* **2002**, *1*, 19–25.
- Zhuravlev, K.; Traikov, K.; Dong, Z.; Xie, S.; Song, Y.; Liu, Z. *Phys. Rev. B* **2010**, *82*, 064116.
- Ciabini, L.; Santoro, M.; Bini, R.; Scheettino, V. *J. Chem. Phys.* **2002**, *116*, 2928–2935.
- Katrusiak, A.; Podsiadzo, M.; Budzianowski, A. *Crystal Growth Des.* **2010**, *10*, 3461–3465.
- Pruzan, P.; Chervin, J. C.; Thiery, M. M.; Itie, J. P.; Besson, J. M. *J. Chem. Phys.* **1990**, *92*, 6910–6915.
- Thiery, M. M.; Besson, J. M.; Bribes, J. L. *J. Chem. Phys.* **1992**, *96*, 2633–2654.
- Ciabini, L.; Santoro, M.; Bini, R.; Scheettino, V. *J. Chem. Phys.* **2001**, *115*, 3742–3749.
- Pravica, M.; Grubor-Urosevic, O.; Hu, M.; Chow, P.; Yulga, B.; Liermann, P. *J. Phys. Chem. B* **2007**, *111*, 11635–11637.
- Wen, X.; Hoffmann, R.; Ashcroft, N. W. *J. Am. Chem. Soc.* **2011**, *133*, 9023–9035.
- Thiery, M. M.; Leger, J. M. *J. Chem. Phys.* **1988**, *89*, 4255–4271.
- Cansell, F.; Fabre, D.; Petit, J.-P. *J. Chem. Phys.* **1993**, *99*, 7300–7304.
- Thiery, M. M.; Rerat, C. *J. Chem. Phys.* **1996**, *104*, 9079–9089.
- Ciabini, L.; Santoro, M.; Gorelli, F. A.; Bini, R.; Scheettino, V.; Rauei, S. *Nat. Mater.* **2007**, *6*, 39–43.
- Ciabini, L.; Santoro, M.; Bini, R.; Scheettino, V. *Phys. Rev. Lett.* **2002**, *88*, 085505.
- Mao, H. K.; Xu, J.; Bell, P. M. *J. Geophys. Res.* **1986**, *91*, 4673–4676.
- Wang, D.; Mittauer, K.; Reynolds, N. *Am. J. Phys.* **2009**, *77*, 1130–1134.
- Wood, R. W. *Phys. Rev.* **1930**, *36*, 1431–1434.
- Casiraghi, C.; Ferrari, A. C.; Robertson, J. *Phys. Rev. B* **2005**, *72*, 085401.
- Bowden, M.; Gardiner, D. J.; Southall, J. M. *J. Appl. Phys.* **1992**, *71*, 521–523.
- Ferrari, A. C.; Robertson, J. *Phys. Rev. B* **2000**, *51*, 14095.
- Wen, X.; Hand, L.; Labet, V.; Yang, T.; Hoffmann, R.; Ashcroft, N. W.; Oganov, A. R.; Lyakhov, A. O. *Proc. Natl. Acad. Sci. U.S.A.* **2011**, *108*, 6833–6837.
- Taguchi, Y.; Yanagiya, K.; Shibuya, I.; Suhara, Y. *Bull. Chem. Soc. Jpn.* **1988**, *61*, 921–925.
- Nagawa, T.; Zama, Y.; Okamoto, Y. *Bull. Chem. Soc. Jpn.* **1984**, *57*, 2035–2036.
- Dziubek, K. F.; Katrusiak, A. *J. Phys. Chem. B* **2004**, *108*, 19089–19092.
- Butcher, E. G.; Weston, J. A.; Gebbie, G. A. *J. Chem. Phys.* **1964**, *41*, 2554–2555.
- Socrates, G. *Infrared and Raman Characteristic Group Frequencies: Tables and Charts*; John Wiley & Sons Ltd.: Chichester, U.K., 2001; p 212.
- Meyer, B. *Chem. Rev.* **1976**, *76*, 367–388.
- Eckert, B.; Albert, H. O.; Jodl, H. J.; Foggi, P. *J. Phys. Chem.* **1996**, *100*, 8212–8219.
- Becucci, M.; Bini, R.; Castellucci, E.; Eckert, B.; Jodl, H. J. *J. Phys. Chem. B* **1997**, *101*, 2132–2137.
- Nakamoto, K. *Infrared and Raman Spectra of Inorganic and Coordination Compounds Part A: Theory and Applications in Inorganic Chemistry*; John Wiley & Sons Ltd.: New York, 2009; p 83.